Acta Geotechnica Slovenica

ALGEBRAIC CONSISTENCY OF ROCKBURST RECORDS FOR UNDERGROUND EXCAVATION

Chukwudi Okonkwo

Department of Mining Engineering, School of Infrastructure, Minerals and Manufacturing Engineering, Federal University of Technology Akure, Akure, Ondo State, Nigeria

Received: 19/06/2024 Revised: 12/08/2024 Accepted: 11/10/2024 Published: 17/11/2024

***Correspondence:** chuokon45@yahoo.com

DOI: 10.68304/gsej2024.a109

ABSTRACT

Rockburst classification often combines circumferential stress and rock strengths with ratios calculated from the same quantities. Conflicting ratio values can describe mechanically incompatible conditions even when a classifier assigns the correct severity grade. Joint compatibility is examined for 344 underground rockburst cases through intervals determined by decimal precision. The stress-concentration factor and two brittleness indices reduce to intersecting admissible intervals for compressive strength, with an independent linear-programming check of the resulting criterion. Fourteen cases are infeasible under half-last-digit allowances. Ten contain mutually incompatible brittleness indices and remain infeasible when the stress and strength intervals are widened by 10%. A fixed 0.005 residual threshold flags substantially more first-index entries, showing that pointwise disagreement and joint infeasibility require separate interpretations. Burial depth is unavailable for 38.08% of the cases and is excluded consistently from classification. Four input representations are compared using a fixed random forest and repeated cross-validation that keeps identical stress–strength–energy profiles within one fold. Recalculating the ratios changes individual predictions but leaves mean accuracy nearly unchanged: 57.99% against 58.11% for the tabulated inputs. The feasibility criterion identifies combinations requiring verification of index definitions and mechanical quantities before calibration.

Keywords: rockburst severity; underground excavation; strength indices; interval feasibility; stress–strength compatibility; grouped validation

1. INTRODUCTION

Excavation redistributes stress around an underground opening and can release stored elastic energy through violent rock failure. Rockburst assessment consequently depends on the relation between boundary stress, intact strength, rock structure and excavation conditions. Support

© 2024 The Author(s). Published under the CC BY 4.0 license.

selection additionally requires estimates of damage mechanisms and energy demand [1]. Analyses of brittle failure around tunnels establish the importance of stress concentration and strength interpretation [2], while histories of intense tunnel rockbursts demonstrate the influence of the surrounding geological and construction conditions [3].

Rockburst assessment combines observations with different mechanical meanings. Intact strength tests characterize specimen failure under specified laboratory conditions, boundary-stress calculations describe an excavation-induced loading state, and a severity label summarizes an event or its consequences. Reviews of rockburst evaluation distinguish empirical, numerical, statistical and intelligent approaches and show the diversity of data used in those approaches [4]. Experimental reviews also distinguish controlled laboratory observations from theoretical and numerical descriptions of burst mechanisms [5]. Combining such evidence can be useful, but it also creates opportunities for a derived index to be detached from its defining measurements. Before evaluating prediction quality, a basic requirement is that the assembled quantities can describe one mechanically possible input state.

Predictive rockburst studies have used stress, strength and derived indices together in supervised classification [6]. Support-design assessments in burst-prone ground additionally emphasize the mechanical interpretation of damage and the conditions at the excavation boundary [7]. These two uses of evidence should remain distinguishable. A derived index can be useful for classification while still requiring consistency with the measurements from which it is defined. Conversely, a mechanically consistent feature vector does not establish that the available labels describe all aspects of the failure mechanism or the demand on a support system.

Stress-based severity classifications commonly include a circumferential-stress-to-compressive-strength ratio and two indices calculated from compressive and tensile strengths. These quantities express useful mechanical contrasts, but their algebraic dependence constrains the combinations they can assume. For example, a particular compressive-to-tensile-strength ratio fixes the normalized strength difference exactly. Two incompatible values cannot describe the same positive strength pair. A classifier may nevertheless use both columns and assign a severity grade, without revealing that contradiction.

Mechanical compatibility is separate from the adequacy of an index as a description of burst behaviour. Laboratory investigations of intrinsic strainburst proneness examine stress–strain response and released energy directly [8]. Rock-mass characterisation also requires investigation of discontinuities, strength and deformation behaviour at the scale of the excavation [9]. Agreement among strength ratios is therefore a necessary internal check, while the physical interpretation of each case still depends on its geological and loading conditions.

The use of compressive and tensile strength deserves particular care because the measured tensile value depends on the testing concept and procedure. Reviews of rock tensile strength distinguish the interpretation of direct and indirect measurements and the assumptions involved in each [10]. The same numerical ratio can therefore carry different uncertainty when its denominator comes from different test procedures. More generally, brittleness is not a universally interchangeable scalar description of failure; different definitions emphasize different aspects of mechanical behavior

[11]. The present compatibility analysis does not choose a universally preferred brittleness index. It asks whether the definitions actually used in the table can all be evaluated from a common positive pair of strengths.

Rock-mass strength estimation provides a further scale distinction. Established discussions of rock-mass strength and subsequent development of the Hoek–Brown failure criterion address the transfer from intact properties to a fractured rock mass [12, 13]. The present input-consistency test does not perform that transfer. It checks the shared intact strengths implied by the tabulated index definitions. A feasible solution therefore establishes algebraic compatibility at the stated input level, while uncertainty in rock-mass characterization and the actual excavation stress remains a separate part of the engineering assessment.

The analysis addresses two questions. First, can one positive stress–strength triple satisfy the stress-concentration factor and both brittleness indices simultaneously within allowances for decimal precision? Second, how do alternative treatments of those indices affect classification when severity grades and test cases are held fixed? A discrepancy evaluated at a tabulated point, an infeasible interval combination and a changed prediction are examined separately. Their distinction prevents a small rounding difference from being treated as a mechanical contradiction, or a favourable prediction from being treated as confirmation of an inconsistent input.

The uses and limitations of the Hoek–Brown criterion illustrate why a strength description must be interpreted within its intended mechanical setting [14]. Assessments of numerical-model reliability also distinguish uncertainty in geological inputs from error introduced by the modeling procedure [15]. These perspectives motivate reporting the compatibility result separately from a change in predictive score. Omitting a conflicting index can restore a possible shared-strength description, but does not establish which reported channel was erroneous. A classification improvement after that omission is evidence about the representation used by the model, rather than independent verification of the reconstructed stress or strengths.

This distinction remains important even when the indices are intended only as predictors. Two derived channels can be strongly dependent for physical reasons, while their tabulated values can also violate the exact algebra linking them. The former is expected when they share underlying measurements; the latter requires an explanation involving precision, definitions, transcription or source provenance. Data-preprocessing studies in rockburst assessment demonstrate the relevance of checking the inputs supplied to machine-learning models [16]. Here the check is made explicit through interval feasibility. Rounding allowances are attached to the reported channels before incompatibility is declared, so a contradiction is not inferred solely from the failure of printed decimals to satisfy an identity exactly.

Cross-validation must respect repeated inputs and the dependence relevant to the intended application [17]. Identical mechanical profiles are kept together during partitioning. Project identities are unavailable, so this control prevents exact profile overlap without establishing independence between excavation sites. Predictive comparisons consequently describe sensitivity within the cases considered, rather than forecasting performance for a new tunnel.

Monitoring investigations at Jinping II illustrate the practical connection between excavation conditions, observed rockburst characteristics and microseismic evidence [18]. The engineering consequences extend beyond a change in classification accuracy. Support design under burst conditions must consider failure mechanisms and energy demand [1], whereas brittle-failure analysis around tunnels addresses the interpretation of excavation stress and rock strength [2]. Internal index consistency is a necessary preliminary check for a calculation that claims to use those measurements, but it cannot establish either the correctness of the stress estimate or the adequacy of the support. Likewise, removing a conflicting channel may restore algebraic feasibility without recovering the true original strength. The analysis therefore reports the smallest omissions that restore compatibility as diagnostic alternatives, not as certified corrections. Holding the available cases and grades fixed then isolates how the representation of the same inputs affects the classifier, while grouped validation limits direct overlap between identical mechanical profiles.

The mathematical development provides a shared-strength interval, its necessary and sufficient feasibility condition, and the minimum set of index channels whose omission restores compatibility. Worked cases distinguish incompatible brittleness definitions from smaller stress-ratio discrepancies. The classification comparison then separates changes in mechanical representation from changes in agreement with the severity grades.

2. ROCKBURST CASES AND MECHANICAL QUANTITIES

2.1 STRESS, STRENGTH, ENERGY AND SEVERITY

Rockburst intensity has been assessed using maximum circumferential stress, uniaxial compressive and tensile strengths, elastic-energy storage and burial depth [16]. The cases examined here comprise four severity grades: none, light, moderate and strong. Their respective counts are 50, 98, 123 and 73. The analysis retains those grades throughout the compatibility checks and classification comparisons.

The mechanical quantities and their ranges appear in Table 1. Circumferential stress extends from 2.6 to 297.8 MPa, compressive strength from 20.0 to 304.2 MPa and tensile strength from 0.4 to 22.6 MPa. The elastic energy index spans 0.81–30.0. Three additional columns contain ratios defined by the stresses and strengths. Including burial depth, the eight predictors therefore contain at most five underlying physical quantities when the index definitions hold; excluding depth leaves four. The ratios can still affect how a classifier partitions that information. Index ranges precede recalculation.

Among the 213 cases with known burial depth, the conditional cumulative distributions differ across severity grades (Figure 1). The respective sample counts are 37, 66, 68 and 42; their median depths are 510, 696, 720 and 841.5 m. Each curve divides the number of known depths at or below a given value by the number available within that grade. These distributions do not include an estimate for any absent depth.

TABLE 1. MECHANICAL QUANTITIES USED IN ROCKBURST CLASSIFICATION.

Quantity	Unit	Range	Definition or role
σ_θ	MPa	2.6–297.8	Maximum circumferential stress
σ_c	MPa	20.0–304.2	Uniaxial compressive strength
σ_t	MPa	0.4–22.6	Uniaxial tensile strength
S (SCF)	–	0.05–4.87	σ_θ/σ_c
B_1	–	0.15–80.0	σ_c/σ_t
B_2	–	0.43–1.00	$(\sigma_c-\sigma_t)/(\sigma_c+\sigma_t)$
W_{et}	–	0.81–30.0	Elastic-to-dissipated energy ratio at loading to $0.8\sigma_c$
D	m	100–2372	Burial depth
g	ordinal	0, 1, 2, 3	None, light, moderate and strong rockburst

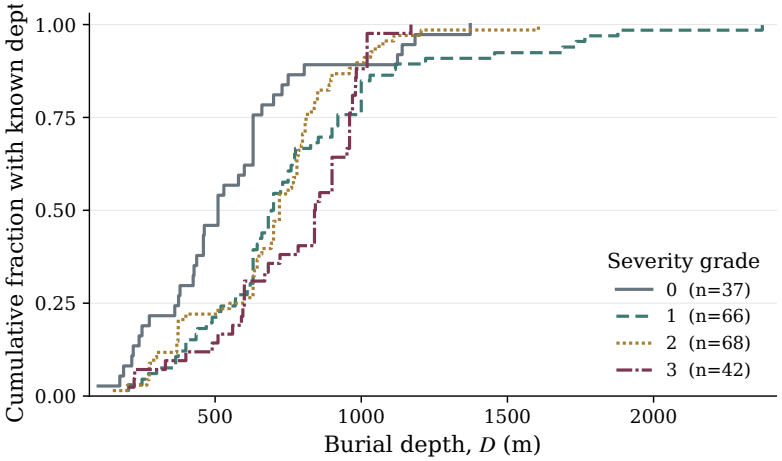

FIGURE 1. BURIAL-DEPTH DISTRIBUTIONS WITHIN THE FOUR SEVERITY GRADES.

2.2 CASE VERIFICATION AND DEPENDENCE

Each numerical entry was checked through two independent table-reading procedures, followed by visual inspection of the cases failing the compatibility criterion. Case numbers and decimal precision were retained so that every diagnostic corresponds to an identifiable mechanical combination. No outlier was removed, no severity grade was changed and unavailable depths were not imputed.

Circumferential stress, both strengths and the energy index are positive and available for every case. Their joint values define 342 distinct profiles. Cases 165/192 share the same four quantities, as do cases 180/187, with matching severity within each pair. These pairs are retained and assigned wholly to one cross-validation fold. They create no contradictory grade assignment for an identical four-variable profile.

The compatibility calculation covers every case considered and needs no assumption of independent random sampling. Predictive interpretation is more restricted. Neither the number of rows nor the number of distinct mechanical profiles establishes the number of independent excavation sites. Project identities, sampling probabilities and complete acquisition conditions are unavailable. Case-specific specimen geometry, loading rate, circumferential-stress estimation, excavation sequence and monitoring history therefore cannot be resolved uniformly. The calculations assess numerical compatibility and classification sensitivity under those limits.

3. JOINT FEASIBILITY OF STRESS AND STRENGTH INDICES

3.1 PRINTED PRECISION AND THE ALGEBRAIC CONSTRAINTS

For positive stress and strength values $\theta = \sigma_\theta$, $c = \sigma_c$ and $t = \sigma_t$, define

$$S = \frac{\theta}{c}, \qquad B_1 = \frac{c}{t}, \qquad B_2 = \frac{c - t}{c + t}. \tag{1}$$

A pointwise residual subtracts the value calculated from the tabulated stress and strength values from the tabulated index. As an initial diagnostic only, a residual magnitude above 0.005 is counted for each index. This fixed tolerance is dimensionless and corresponds to half a hundredth; it does not account for uncertainty in the stress and strength values and is not used to declare a record jointly inconsistent.

For a decimal value with d digits after its decimal point, let $h = 0.5 \times 10^{-d}$. Its nominal interval is $[x - h, x + h]$, truncated to positive values for the stress and strength quantities. An integer token therefore receives $h = 0.5$, while a token such as 0.90 receives $h = 0.005$. This is a declared half-last-digit allowance. It is not a measured sensor error, and omitted trailing zeros make it a deliberately permissive convention for some entries. A sensitivity check instead assigns every input stress a common half-width of 0.005 MPa.

Write the stress and strength intervals as $[\theta_-, \theta_+]$, $[c_-, c_+]$ and $[t_-, t_+]$, and the index intervals as $[s_-, s_+]$, $[b_-, b_+]$ and $[v_-, v_+]$. In this collection $s_- > 0$ and $v_- > -1$. A record is jointly feasible if one common triple (θ, c, t) within the stress and strength intervals satisfies all three index intervals. Checking each index separately is insufficient because the same strength values appear in several definitions.

3.2 REDUCTION TO ONE SHARED-STRENGTH INTERVAL

The two brittleness indices satisfy

$$B_2 = \frac{B_1 - 1}{B_1 + 1}, \qquad B_1 = F(B_2) = \frac{1 + B_2}{1 - B_2}. \tag{2}$$

The function F is increasing for $-1 < B_2 < 1$. Define the ratio bounds implied by the second index as

$$f_- = F(v_-), \qquad f_+ = \begin{cases} F(v_+), & v_+ < 1, \\ +\infty, & v_+ \geq 1. \end{cases} \tag{3}$$

The infinite upper endpoint handles a printed value of 1.00 without treating it as an exact, physically attainable normalized difference. The common admissible interval for c/t is

$$R_- = \max(b_-, f_-), \qquad R_+ = \min(b_+, f_+). \tag{4}$$

If $R_- > R_+$, the two tabulated brittleness indices are intrinsically incompatible: changing the input stresses cannot make them both correct within their specified index intervals.

Otherwise, all constraints reduce to an intersection for compressive strength,

$$C_- = \max\left(c_-, R_- t_-, \frac{\theta_-}{s_+}\right), \qquad C_+ = \min\left(c_+, R_+ t_+, \frac{\theta_+}{s_-}\right). \tag{5}$$

The exact real-arithmetic criterion is

$$\mathcal{F} = 1 \quad \Longleftrightarrow \quad R_- \le R_+ \text{ and } C_- \le C_+. \tag{6}$$

Necessity follows by substituting any admissible triple into the ratio bounds. For sufficiency, choose c in $[C_-, C_+]$. The interval $[c/R_+, c/R_-]$ intersects $[t_-, t_+]$, so an admissible t can be selected. Independently, $[s_- c, s_+ c]$ intersects $[\theta_-, \theta_+]$, so an admissible θ can be selected. These choices satisfy all three definitions with the same c. Endpoint conventions handle an infinite R_+ in the usual limiting sense.

An independent numerical formulation checks the same result using linear programming. For example, the SCF constraints become $\theta - s_- c \ge 0$ and $s_+ c - \theta \ge 0$. The brittleness constraints are

$$c - b_- t \ge 0, \qquad b_+ t - c \ge 0, \tag{7}$$

$$(1 - v_-)c - (1 + v_-)t \ge 0, \qquad (1 + v_+)t - (1 - v_+)c \ge 0. \tag{8}$$

These linear inequalities, together with the stress and strength bounds, form a feasibility problem with three unknowns. SciPy's HiGHS interface is used for the numerical check [19]. The analytical calculation and linear program agree for every audited record, uncertainty setting and index-omission combination. Numerical comparisons in the interval calculation use a 10^{-12} endpoint allowance; the linear program uses 10^{-9} primal and dual feasibility tolerances.

For a direct measure of brittleness-interval separation, define $Q = R_-/R_+$ when both endpoints are positive and finite. A value above unity identifies a nonempty gap between the two required ratio intervals. This dimensionless quantity describes algebraic separation, not a probability of error or an estimate of rockburst intensity.

To compare the scales of point discrepancies, let $e_j = |j_{\text{tab}} - j_{\text{calc}}|/h_j$ for $j \in \{S, B_1, B_2\}$, where h_j is that index's half-last-digit allowance. The display coordinate $\log_{10}(1 + e_j)$ preserves zero while compressing large discrepancies. This diagnostic uses the stress and strength point values; unlike Eq. (6), it does not propagate their intervals.

3.3 UNCERTAINTY SENSITIVITY AND MINIMUM OMISSION

An additional relative allowance ρ expands each input interval to

$$x_\pm(\rho) = x \pm (h_x + \rho x), \qquad \rho \in \{0, 0.01, 0.05, 0.10\}, \tag{9}$$

with a positive lower bound. Index intervals remain unchanged. The added allowances are sensitivity choices, not estimates of field measurement accuracy. Since Eq. (4) depends only on the index intervals, intrinsic brittleness incompatibility cannot be resolved by increasing ρ.

For an infeasible record, each subset of the three index channels is considered in turn. The minimum omission count is

$$k^* = \min_{A \subseteq \{S, B_1, B_2\}} |A| \quad \text{subject to feasibility of the retained channels } \{S, B_1, B_2\} \setminus A. \tag{10}$$

Omitting B_1 removes its contribution to Eq. (4); omitting B_2 removes the bounds from Eq. (3); omitting SCF removes the SCF-derived bounds in Eq. (5). All minimum-cardinality solutions are retained. This diagnostic identifies which index channels must be set aside when the stress and strength intervals are held fixed. It does not establish which measurement or transcription is wrong.

Case 20 has $\theta = 54.2$ MPa, $c = 134$ MPa, $t = 9.1$ MPa, $S = 0.4$, $B_1 = 0.15$, $B_2 = 0.87$, $W_{et} = 7.1$ and grade 2; depth is absent. Direct calculation gives

$$\frac{54.2}{134} = 0.404478, \qquad \frac{134}{9.1} = 14.725275, \qquad \frac{134 - 9.1}{134 + 9.1} = 0.872816. \tag{11}$$

The printed first-index interval is $[0.145, 0.155]$. The second-index interval is $[0.865, 0.875]$, implying

$$\frac{c}{t} \in \left[\frac{1.865}{0.135}, \frac{1.875}{0.125}\right] = [13.814815, 15.000000]. \tag{12}$$

Thus $R_- = 13.814815 > R_+ = 0.155$. The contradiction exists before any input uncertainty is considered. Omitting the first-index channel restores feasibility with the other channels and stress and strength intervals retained. Using the ratio in Eq. (11) adopts the tabulated strengths without changing the severity grade.

Case 170 illustrates a different situation. Its values include $\theta = 26.9$ MPa, $c = 62.8$ MPa, $t = 2.1$ MPa and $S = 0.42$. Their half-last-digit intervals require

$$c \geq \frac{26.85}{0.425} = 63.176471 \text{ MPa}, \qquad c \leq 62.85 \text{ MPa}. \tag{13}$$

The SCF constraint is therefore infeasible under that convention. A 1% additional input allowance makes this record feasible. Unlike case 20, the disagreement is not an intrinsic contradiction between the brittleness indices. These two examples show why the mathematical diagnosis must precede an interpretation of its cause.

The stress plane in Figure 2 locates the bounds for case 170 relative to $0.415c \leq \theta \leq 0.425c$. The narrow rectangle is disjoint from this admissible band, whereas the 1% expanded rectangle intersects it. The projection isolates the SCF restriction; feasibility of the remaining brittleness restrictions is checked with the full three-variable criterion.

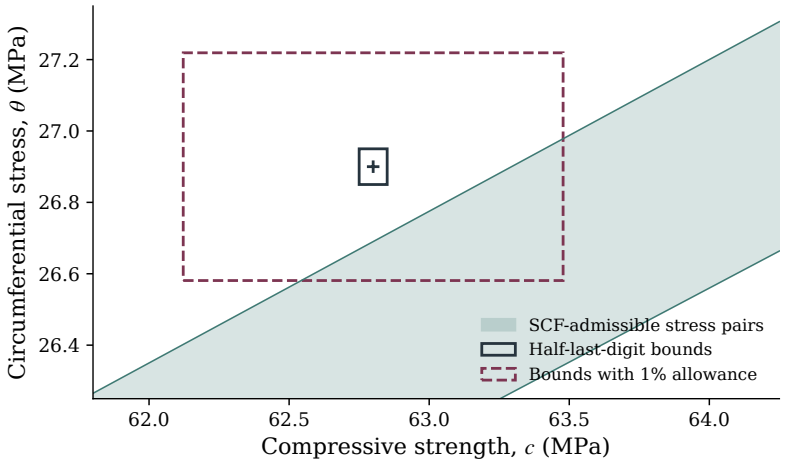

FIGURE 2. STRESS BOUNDS AND SCF ADMISSIBILITY FOR CASE 170.

4. ROCKBURST SEVERITY CLASSIFICATION

4.1 FOUR FEATURE REPRESENTATIONS

A fixed random forest compares the four input representations [20]. The severity grades are fixed across four alternatives. R7 retains the seven complete tabulated predictors $(\theta, c, t, S, B_1, B_2, W_{et})$. C7 recalculates all three indices through Eq. (1) while retaining the tabulated stress and strength values. T7 recalculates only the channels identified by the minimum-omission diagnostic in infeasible records, leaving every other tabulated entry unchanged. P4 uses only (θ, c, t, W_{et}).

All infeasible cases have a unique minimum-omission set, so T7 does not require a tie-breaking choice. C7 and T7 express the consequences of adopting the tabulated strengths in the ratio definitions. Comparing them separates recalculation of every index from a change targeted to the identified incompatibilities. P4 tests whether deterministic ratios add useful representation for this learner despite adding no independent physical information.

Depth is excluded from every classifier, retaining all 344 records and avoiding unverified depth imputation. It is still included in the coverage audit. The absence of depth limits the physical completeness of every classifier equally. The comparison therefore leaves the effect of burial depth unresolved.

4.2 PARTITIONING AND EVALUATION

Identical (θ, c, t, W_{et}) tuples define 342 groups. StratifiedGroupKFold assigns each group wholly to one of five folds. With $s_0 = 20231118$, the ten partitions use seeds $s_0 + r$, where $r = 0, \ldots, 9$. All representations receive the same training and test indices within each partition. The model seed is $s_0 + 100r + f$, with fold index $f = 0, \ldots, 4$.

Each forest contains 300 trees, uses all available predictors at each candidate split, has a minimum leaf size of two and uses balanced class weights calculated from the training fold. Other settings follow scikit-learn 1.8.0 defaults [21]. No hyperparameter search, oversampling, outlier removal or

label-based imputation is performed. All recalculations are row-local algebraic operations and do not use the held-out labels. The fixed settings isolate representation sensitivity within this classifier.

Each record receives one out-of-fold prediction per representation in each repeat. Accuracy, balanced accuracy, macro F1 and absolute grade error are calculated from the held-out predictions in each repeat and summarized over the ten partitions. With $n = 344$ and four classes, the classification measures include

$$\text{Accuracy} = n^{-1} \sum_i \mathbf{1}\{\widehat{g}_i = g_i\}, \tag{14}$$

$$\text{Balanced accuracy} = \frac{1}{4} \sum_{j=0}^{3} \frac{TP_j}{TP_j + FN_j}, \tag{15}$$

$$\text{Macro F1} = \frac{1}{4} \sum_{j=0}^{3} \frac{2TP_j}{2TP_j + FP_j + FN_j}, \tag{16}$$

$$\text{MAE}_g = n^{-1} \sum_i |\widehat{g}_i - g_i|. \tag{17}$$

The ordinal error assigns one unit to adjacent grades for descriptive purposes; those units do not imply equal increments of physical damage. Strong cases assigned grades 0 or 1 are also counted. Repeats share the same records and are dependent. Their range measures partition sensitivity and is not a confidence interval or evidence of independent replication.

For two representations A and B, let G count records incorrectly classified by A but correctly classified by B, and let L count the converse. The paired accuracy change is

$$\Delta\text{Accuracy} = \frac{G - L}{344}. \tag{18}$$

If W counts predictions that change grade but remain incorrect, the number of changed predictions is $C = G + L + W$. For $C > 0$, the fractions $(G/C, L/C, W/C)$ sum to unity and locate one repeat in a ternary composition plot. Pooling these counts across repeats weights each change equally; it does not create independent observations. The paired counts distinguish changed predictions from net improvement. Cases from one project may still occupy different folds because project identities are unavailable.

5. RESULTS

5.1 CONSISTENCY AT THE POINT AND INTERVAL LEVELS

The pointwise 0.005 check flags 17 SCF entries, 102 first-brittleness-index entries and no second-brittleness-index entries. Under the joint half-last-digit criterion, 330 records are feasible and 14 are infeasible. The latter represent $14/344 = 4.07\%$ of the cases. Marginal checks flag ten records for SCF and ten for B_1, with six records shared between those sets. No record fails the B_2

marginal check alone. Thus a column can agree individually with the stress and strength intervals while disagreeing with another derived column.

The normalized point discrepancies in Figure 3 differ substantially between index channels. The horizontal reference denotes one index half-last-digit. Hollow diamonds identify jointly infeasible cases; small deviations in a single channel neither establish nor exclude joint feasibility. The violin widths describe the distribution of $\log_{10}(1 + e_j)$, with horizontal jitter used only to separate overlapping points.

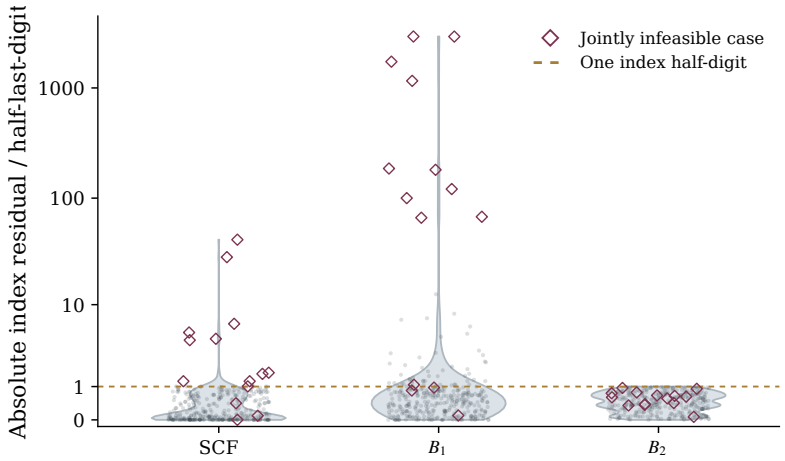

FIGURE 3. RATIO DEVIATIONS RELATIVE TO HALF-LAST-DIGIT PRECISION.

Ten records have disjoint B_1 and B_2 ratio intervals (Figure 4). This is a stronger statement than a large residual at printed point values. It establishes incompatibility under the specified index allowances even if the stress and strength intervals were widened arbitrarily. Conversely, a large number of small point residuals can be compatible with the adopted printed-precision intervals. Of the 102 point-flagged B_1 entries, only ten fail its marginal interval test. The remaining 92 cannot be classified as inconsistent by that permissive interval convention; this does not certify their measurement accuracy.

The separation factor ranges from 1.0575 in case 97 to 89.1278 in cases 20 and 21; case 288 has $Q = 16.9787$. The logarithmic stems in Figure 4 distinguish narrow interval separation from the much larger discrepancies, without attributing a cause to either.

The complete set of jointly infeasible records and minimum omissions appears in Table 2. Eight records require one channel to be omitted: four SCF and four B_1. Six require both SCF and B_1. These solutions are unique with the stress and strength intervals fixed; identifying the erroneous quantity requires checking the mechanical entries and their definitions. The individual case tiles in Figure 5 encode the omission category by position and severity by colour. All six cases requiring both channels have grade 1; the SCF-only category spans grades 1–3. Each tile represents one case rather than a frequency estimate for an excavation population. Severity grades remain fixed.

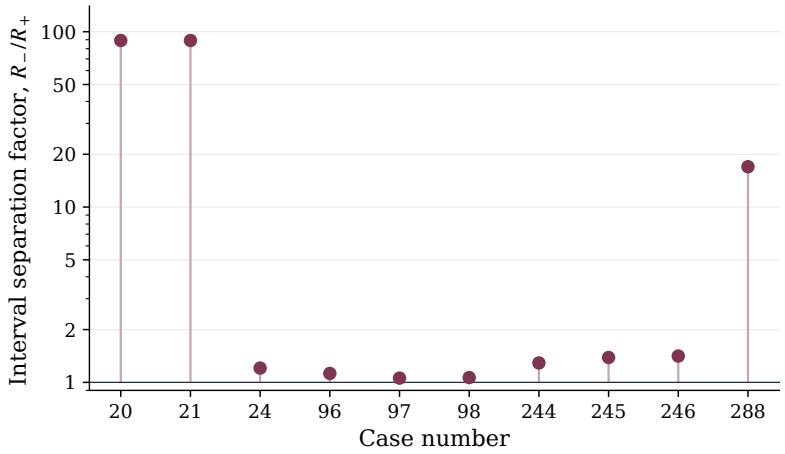

FIGURE 4. SEPARATION BETWEEN INCOMPATIBLE BRITTLENESS INTERVALS.

TABLE 2. COMPLETE LIST OF INFEASIBLE RECORDS UNDER HALF-LAST-DIGIT ALLOWANCES.

Case ID	Grade	Minimum omitted channel(s)	Intrinsic B_1–B_2 conflict
20	2	B_1	Yes
21	2	B_1	Yes
24	2	B_1	Yes
96	1	SCF and B_1	Yes
97	1	SCF and B_1	Yes
98	1	SCF and B_1	Yes
170	1	SCF	No
175	2	SCF	No
189	2	SCF	No
190	3	SCF	No
244	1	SCF and B_1	Yes
245	1	SCF and B_1	Yes
246	1	SCF and B_1	Yes
288	0	B_1	Yes

5.2 SENSITIVITY TO THE PRECISION CONVENTION

Adding a 1% input allowance reduces joint failures from 14 to ten. The count remains ten at 5% and 10%. The persistent records are exactly those with intrinsic brittleness conflicts, as expected from Eq. (4). The four disappearing failures involve SCF alone under the minimum-omission diagnosis.

Assigning every input stress a uniform 0.005 MPa half-width gives 31 jointly infeasible records while retaining the half-last-digit index allowances. This alternative treats integer and single-decimal stress entries much more tightly. The difference confirms that an infeasibility count must state its precision convention. Neither convention is a substitute for metrological uncertainty supplied by the measurement programme. The intrinsic contradictions are the portion that cannot be resolved merely by changing input precision.

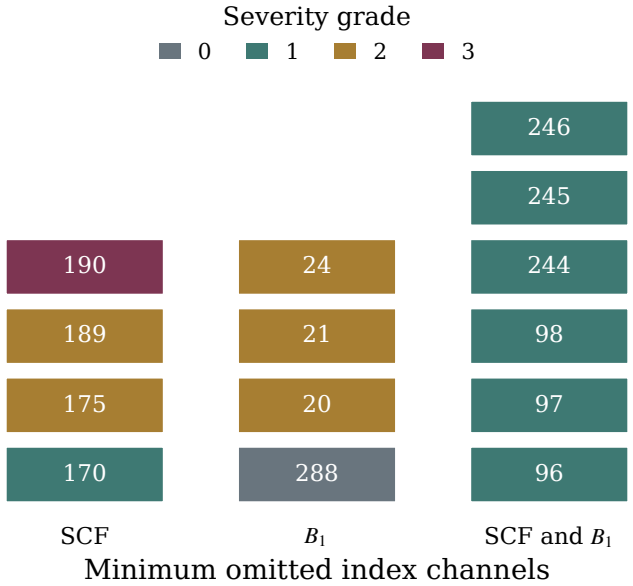

FIGURE 5. MINIMUM INDEX OMISSIONS RESTORING JOINT FEASIBILITY.

5.3 DEPTH COVERAGE AND REPEATED PROFILES

Depth is missing in 131 of 344 records (38.08%). The absent-depth fraction differs across severity grades: 26.00% for none, 32.65% for light, 44.72% for moderate and 42.47% for strong rockburst. These are descriptive differences. They do not identify the mechanism generating missing values or establish that severity causes missingness.

The two repeated stress–strength–energy profiles reduce the number of distinct input groups to 342. Because both pairs have consistent labels, they create no exact label contradiction. Grouping keeps each pair wholly within a training or test fold. This safeguard does not identify near-duplicates, multiple records from one mine, or investigations sharing an event.

5.4 PREDICTION SENSITIVITY WITHOUT RELABELING

The four representations are compared in Table 3. Mean accuracy is 58.11% for R7, 58.14% for T7, 57.99% for C7 and 56.92% for P4. The full C7 recalculation changes an average of 14.2 predictions per repeat relative to R7, but its average gains and losses are 5.8 and 6.2 correct classifications. Therefore its mean accuracy change is $100(-0.4/344) = -0.1163$ percentage points. The joint distribution of accuracy and ordinal error is displayed in Figure 6. Each small symbol denotes one repeat; the larger hollow symbols mark the means. Convex hulls delimit the observed repeat values and are not confidence regions or bounds on future performance. Accuracy ranges span ten dependent partitions and are not confidence intervals. Strong-to-low counts refer to the 73 grade-3 records assigned grade 0 or 1 in one repeat.

The targeted T7 treatment changes an average of 10.7 predictions per repeat, with 4.7 gains and 4.6 losses. Its mean accuracy change is only 0.0291 percentage points. Changes span both signs across the ten partitions. Thus neither wholesale recalculation nor the targeted treatment yields a

material accuracy gain under the specified evaluation. Mean balanced accuracies for R7, T7, C7 and P4 are 59.44%, 59.44%, 59.22% and 58.52%, respectively.

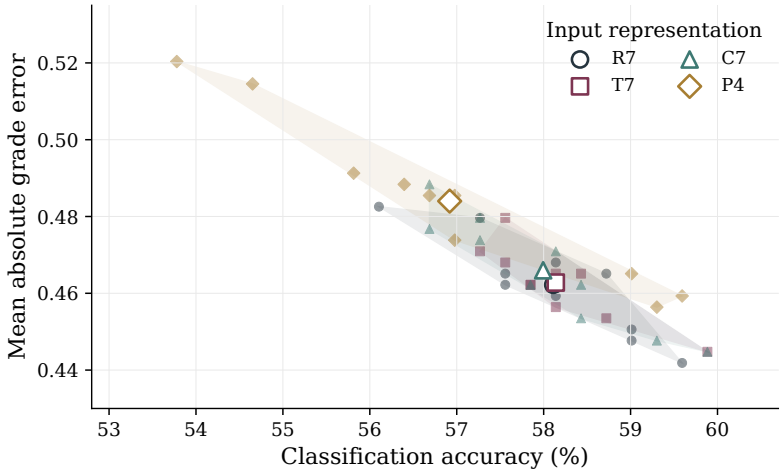

FIGURE 6. CLASSIFICATION ACCURACY AND ORDINAL ERROR ACROSS REPEATED PARTITIONS.

TABLE 3. REPEATED GROUPED CROSS-VALIDATION WITH THE SEVERITY GRADES.

Input	Mean accuracy	Accuracy range	Macro F1	Grade MAE	Strong-to-low
	(%)	(%)			mean count
R7	58.11	56.10–59.59	0.597	0.462	2.2
T7	58.14	57.27–59.88	0.597	0.463	2.0
C7	57.99	56.69–59.88	0.595	0.466	2.2
P4	56.92	53.78–59.59	0.585	0.484	2.9

C7 and P4 contain the same stress–strength–energy information, but their mean accuracies differ by 1.08 percentage points. This difference reflects the learner's representation of decision boundaries, not the acquisition of new physical measurements. Similarly, an algebraically infeasible entry may act as an accidental predictor of a case-dependent grade. Its usefulness to a classifier does not make the entry mechanically coherent. Uncertainty in the severity descriptions and unavailable site conditions remains after recalculation.

The R7 confusion pattern in Figure 7 retains the ordering of the severity grades. Circle area is proportional to the mean count across the ten out-of-fold prediction sets, and colour denotes absolute grade difference. Counts below two remain visible without numerical labels. Adjacent-grade errors dominate: the grade-2 to grade-1 and grade-3 to grade-2 cells average 23.2 and 31.7 cases per repeat. For grade 3, the combined mean count assigned grades 0 or 1 is 2.2. These are repeated predictions of the same cases, rather than independent additional observations.

The composition of C7 changes relative to R7 is shown in Figure 8. Across the ten repeats, 142 predictions change: 58 become correct, 62 become incorrect and 22 change between incorrect grades. Their pooled fractions are 40.85%, 43.66% and 15.49%. The triangular grid advances in increments of 20 percentage points along each component. Each filled point represents one repeat and the hollow diamond combines its constituent counts with those of the other repeats. This display conditions on a changed prediction; it does not describe the fraction of all cases correctly

classified. The prediction remains unchanged in every repeat for 260 cases.

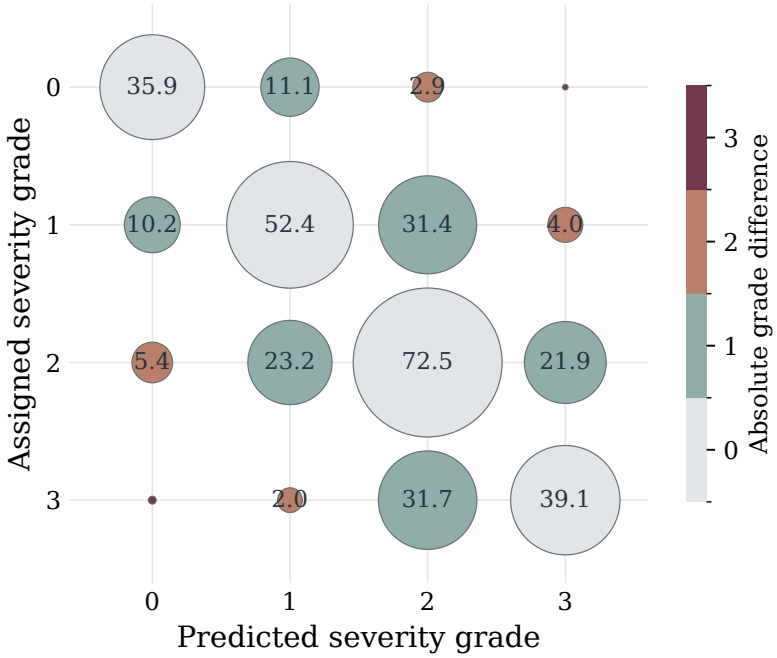

FIGURE 7. MEAN OUT-OF-FOLD CONFUSION FOR THE TABULATED-INPUT CLASSIFIER.

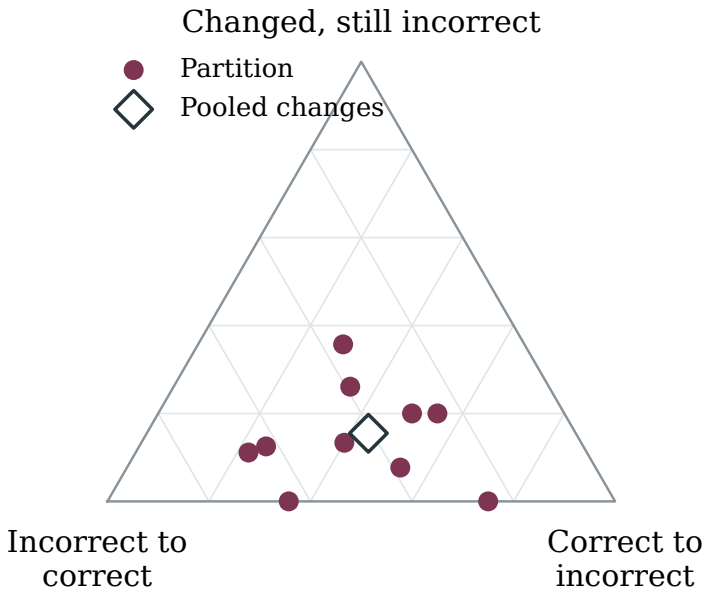

FIGURE 8. COMPOSITION OF PREDICTION CHANGES AFTER COMPLETE RATIO RECALCULATION.

6. GEOTECHNICAL INTERPRETATION AND UNCERTAINTY

6.1 CHECKING MECHANICAL INPUTS BEFORE CLASSIFICATION

Disjoint intervals for two indices describing the same strength ratio require verification of the numerical entries or their definitions. Such a combination cannot receive a consistent mechanical interpretation simply because a classifier assigns a plausible severity grade. The feasibility calculation identifies this condition before statistical fitting, while retaining the case and its assigned grade.

The minimum-omission result directs that verification. A single-channel solution identifies an index whose exclusion is sufficient when the stress and strength intervals remain fixed. A two-channel solution establishes that excluding either channel alone leaves a contradiction. The appropriate next step is to check the stress estimate, strength values, units and index definitions together. The table alone cannot determine whether a disagreement arose through transcription, a different loading condition or a different index convention.

Feasible combinations also require geotechnical judgement. Agreement among the ratios does not verify circumferential-stress estimation, rock-mass structure or the severity description. Excavation geometry, discontinuities, unloading sequence and monitoring information are absent from the four complete predictors. Their omission limits the interpretation of a historical severity class for support planning or warnings during tunnel construction.

The paired classification comparison illustrates why physical compatibility and predictive agreement require different checks. Both complete recalculation and targeted recalculation have little net effect on accuracy, although individual predictions change. A learner can respond to the numerical placement of a value without resolving whether that value satisfies a mechanical definition. Verification of index compatibility must therefore be assessed directly rather than inferred from the ranking of classifier scores.

6.2 DECIMAL PRECISION AND PHYSICAL INTERPRETATION

The interval criterion is necessary and sufficient for the stated positive bounds and ratio definitions in real arithmetic. Agreement with the independent linear program checks its numerical implementation. The criterion establishes admissibility within those bounds; verification of the underlying stress and strength measurements remains a separate requirement.

A displayed integer may be an exact value, a rounded measurement or a number whose trailing zeros were omitted. Half-last-digit allowances accommodate the latter two possibilities permissively. Uniform hundredth-MPa bounds impose a tighter convention and produce more infeasible combinations. Neither convention specifies instrument accuracy. Incompatibility between the two brittleness intervals is stronger because it persists regardless of how far the stress and strength bounds are widened. The additional relative allowances in Eq. (9) describe this sensitivity and have no status as construction acceptance tolerances.

The minimum omitted channels should also be interpreted conditionally. Stress and strength values are restricted to their designated intervals during the diagnosis. Revisiting a measurement definition or a different underlying strength value could change which channel must be omitted. Recalculated indices are consequently conditional alternatives based on the tabulated strengths, rather than new physical measurements.

7. CONCLUSION

The stress-concentration factor and two brittleness indices can be checked simultaneously through one admissible interval for compressive strength. The resulting condition separates arithmetic disagreement at tabulated values from the stronger absence of any compatible stress–strength triple. Minimum channel omission identifies which index constraints must be relaxed when the mechanical input bounds are held fixed.

The decisive inconsistencies concern mutually incompatible brittleness ratios. These survive widening of the stress and strength bounds, whereas smaller SCF discrepancies depend on the decimal-precision allowance. The distinction prevents a uniform residual threshold from being interpreted as a direct measure of physical error.

Recalculating index values has little effect on mean classification accuracy, despite changes in individual held-out predictions. Mechanical compatibility and agreement with severity grades consequently remain separate requirements. For underground excavation assessment, the criterion provides a preliminary check of stress–strength inputs before calibration and interpretation. Support selection and field warnings additionally require geological, construction and monitoring evidence.

CONFLICTS OF INTEREST

The author declares that they have no conflicts of interest related to this research.

DATA AVAILABILITY

The data supporting the findings of this study are available from the corresponding author upon reasonable request.

FUNDING INFORMATION

The author received no external funding for this research.

REFERENCES

1. Kaiser PK, Cai M. Design of rock support system under rockburst condition. *Journal of Rock Mechanics and Geotechnical Engineering*. 2012;4(3):215–227. .
2. Martin CD, Kaiser PK, McCreath DR. Hoek-Brown parameters for predicting the depth of brittle failure around tunnels. *Canadian Geotechnical Journal*. 1999;36(1):136–151. .
3. Zhang C, Feng XT, Zhou H, Qiu S, Wu W. Case histories of four extremely intense rockbursts in deep tunnels. *Rock Mechanics and Rock Engineering*. 2012;45(3):275–288. .
4. Zhou, J.; Li, X.; Mitri, H.S. (2018). Evaluation method of rockburst: State-of-the-art literature review. *Tunnelling and Underground Space Technology*, 81, 632–659. https://doi.org/10.1016/j.tust.2018.08.029.
5. He, M.; Cheng, T.; Qiao, Y.; Li, H. (2023). A review of rockburst: Experiments, theories, and simulations. *Journal of Rock Mechanics and Geotechnical Engineering*, 15(5), 1312–1353. https://doi.org/10.1016/j.jrmge.2022.07.014.
6. Zhou, J.; Li, X.; Shi, X. (2012). Long-term prediction model of rockburst in underground openings using heuristic algorithms and support vector machines. *Safety Science*, 50(4), 629–644. https://doi.org/10.1016/j.ssci.2011.08.065.
7. Kaiser, P.K.; Cai, M. (2013). Critical review of design principles for rock support in burst-prone ground – time to rethink!. *Ground Support 2013: Proceedings of the Seventh International Symposium on Ground Support in Mining and Underground Construction, Australian Centre for Geomechanics, Perth*, 3–37. https://doi.org/10.36487/ACG_rep/1304_01_Kaiser.
8. Shi L, Li CC, Zhang X, Feng XT. Experimental verification of the intrinsic strainburst proneness of various rock types. *Bulletin of Engineering Geology and the Environment*. 2023;82:119. .
9. Ocepek D. New trends in rock mass characterisation for designing geotechnical structures. *Acta Geotechnica Slovenica*. 2005;2(2):39–51.
10. Perras, M.A.; Diederichs, M.S. (2014). A Review of the Tensile Strength of Rock: Concepts and Testing. *Geotechnical and Geological Engineering*, 32(2), 525–546. https://doi.org/10.1007/s10706-014-9732-0.
11. Singh, S.P. (1986). Brittleness and the mechanical winning of coal. *Mining Science and Technology*, 3(3), 173–180. https://doi.org/10.1016/s0167-9031(86)90305-1.
12. Hoek, E.; Brown, E.T. (1997). Practical estimates of rock mass strength. *International Journal of Rock Mechanics and Mining Sciences*, 34(8), 1165–1186. https://doi.org/10.1016/s1365-1609(97)80069-x.
13. Hoek, E.; Brown, E.T. (2019). The Hoek–Brown failure criterion and GSI – 2018 edition. *Journal of Rock Mechanics and Geotechnical Engineering*, 11(3), 445–463. https://doi.org/10.1016/j.jrmge.2018.08.001.
14. Eberhardt, E. (2012). The Hoek–Brown Failure Criterion. *Rock Mechanics and Rock Engineering*, 45(6), 981–988. https://doi.org/10.1007/s00603-012-0276-4.
15. Wiles, T.D. (2006). Reliability of numerical modelling predictions. *International Journal of Rock Mechanics and Mining Sciences*, 43(3), 454–472. https://doi.org/10.1016/j.ijrmms.2005.08.001.

16. Li J, Fu H, Hu K, Chen W. Data preprocessing and machine learning modeling for rockburst assessment. *Sustainability*. 2023;15(18):13282. .

17. Roberts DR, Bahn V, Ciuti S, Boyce MS, Elith J, Guillera-Arroita G, Hauenstein S, Lahoz-Monfort JJ, Schröder B, Thuiller W, Warton DI, Wintle BA, Hartig F, Dormann CF. Cross-validation strategies for data with temporal, spatial, hierarchical, or phylogenetic structure. *Ecography*. 2017;40(8):913–929. .

18. Ma, T.H.; Tang, C.A.; Tang, L.X.; Zhang, W.D.; Wang, L. (2015). Rockburst characteristics and microseismic monitoring of deep-buried tunnels for Jinping II Hydropower Station. *Tunnelling and Underground Space Technology*, 49, 345–368. `https://doi.org/10.1016/j.tust.2015.04.016`.

19. Virtanen P, Gommers R, Oliphant TE, Haberland M, Reddy T, Cournapeau D, et al. SciPy 1.0: fundamental algorithms for scientific computing in Python. *Nature Methods*. 2020;17:261–272. .

20. Breiman L. Random forests. *Machine Learning*. 2001;45(1):5–32. .

21. Pedregosa F, Varoquaux G, Gramfort A, Michel V, Thirion B, Grisel O, et al. Scikit-learn: machine learning in Python. *Journal of Machine Learning Research*. 2011;12:2825–2830.